[CANCER RESEARCH 63, 3556–3559, July 1, 2003]

In Situ Detection of Neoplastic Transformation and Chemopreventive Effects in Rat Esophagus Epithelium Using Angle-resolved Low-coherence Interferometry[1]

Adam Wax,[2] Changhuei Yang, Markus G. Müller, Ronald Nines, Charles W. Boone, Vernon E. Steele, Gary D. Stoner, Ramachandra R. Dasari, and Michael S. Feld

Department of Biomedical Engineering, Duke University, Durham, North Carolina 27708 [A. W., C. Y.]; G. R. Harrison Spectroscopy Laboratory, Massachusetts Institute of Technology, Cambridge, Massachusetts 02139 [M. G. M., C. W. B., R. R. D., M. S. F.]; The Ohio State University Comprehensive Cancer Center, Columbus, Ohio 43210 [R. N., G. D. S.]; and Division of Cancer Prevention, National Cancer Institute, Bethesda, Maryland 20892 [V. E. S.]

ABSTRACT

We present a quantitative study of the nuclear morphometry of epithelial cells in an animal model of esophageal carcinogenesis. Changes in the size and texture of cell nuclei as a result of neoplastic transformation and chemopreventive action are observed *in situ* using a new optical technique, angle-resolved low-coherence interferometry (a/LCI). The capabilities of a/LCI are demonstrated via quantitative *in situ* measurements of the nuclear morphometry of basal epithelial cells, ~50–100 μm beneath the tissue surface without the need for exogenous contrast agents or tissue fixation. The measurements quantify changes in nuclear size, characterized by average diameter, and nuclear texture, characterized by fractal dimension of the subcellular structures. Using this technique, we observed changes in the morphometry of rat esophageal epithelial cells in response to treatment with the carcinogen *N*-nitrosomethylbenzylamine. In addition, morphometric changes were observed in the esophagi of rats treated with *N*-nitrosomethylbenzylamine and two chemopreventive agents, difluoromethylornithine and perillyl alcohol. These agents induced either apoptosis in the basal epithelium (difluoromethylornithine) or both apoptosis and vacuolation of basal epithelial cells (perillyl alcohol). Vacuolation was associated with cellular toxicity. The light-scattering measurements were compared with histological images of the same tissues. The potential of a/LCI as a noninvasive means to investigate the development of epithelial neoplasia and for tracking the efficacy of chemopreventive agents appears high. This technique also may provide a new screening tool for intraepithelial neoplasia.

INTRODUCTION

Current methods for early detection and diagnosis of cancer rely on histological and cytological examination of tissue or samples from bodily fluids. The extracted sample is fixed, stained, and then examined with the light microscope. This approach has the drawback that the samples must be taken either at random or on the appearance of a visual cue apparent to the clinician.

In its earliest stages, epithelial precancer (preinvasive neoplasia) appears as an abnormal focal proliferation of cells, termed hyperplasia. Hyperplastic lesions may then progress to intraepithelial dysplasia, carcinoma *in situ*, and, eventually, to invasive carcinoma. Histopathological slides of biopsied tissue or cytological smears from surface brushings are graded by the pathologist according to the degree and extent of neoplastic morphological change as seen under the microscope. The grading of neoplasia is a subjective process that is well known for its interobserver variability.

Recently, LSS[3] has been shown to be capable of *in situ* detection of neoplasia (1). This technique yields quantitative information on nuclear morphology in epithelial layers without the need for biopsy and histopathologic evaluation. Application of such noninvasive, nonperturbative techniques provides a unique opportunity to study the biology of neoplastic progression in living tissue, free from the artifacts associated with preparation of a histopathological slide for diagnostic evaluation. Presented here is a study of neoplastic change in a rat model of esophageal tumorigenesis which makes use of an interferometry-based LSS technique known as a/LCI (2).

The a/LCI technique obtains structural information by examining the angular distribution of backscattered light using a single broadband light source. Thus, a/LCI represents an alternative to previous LSS techniques, which examine wavelength-dependent scattering to extract structure. In addition, a/LCI exploits the short coherence length of the light source to achieve optical sectioning, *i.e.*, to selectively probe subsurface layers to construct depth-resolved tomographic images. This method of optical sectioning via coherence gating is also used in optical coherence tomography, a technique used to image structure in living tissues (3, 4). In the studies presented here, this capability has been exploited to selectively study the morphometry of basal cell nuclei, rejecting the light scattered by the suprabasal layers.

This study presents quantitative measurements of nuclear morphometry as biomarkers for detecting and characterizing the degree of neoplastic change. a/LCI is used to measure *in situ*, in the living state, the average size of cell nuclei and parameterize the cyto-nuclear texture of the living tissue cells of rat esophageal epithelium without the need for exogenous staining agents or fixatives. The a/LCI measurements are compared with traditional histopathological images to establish a correlation with the degree of neoplastic transformation. In addition, the data presented demonstrate the potential utility of a/LCI for screening the efficacy of chemopreventive agents by identifying changes in nuclear features in response to exposure to such agents.

MATERIALS AND METHODS

Chemicals. NMBA, with a purity of >99%, was purchased from Ash Stevens, Inc. (Detroit, MI) and solubilized in 20% DMSO. DFMO was obtained from the National Cancer Institute Division of Cancer Prevention and Control Repository (McKesson BioServices, Rockville, MD). POH and DMSO were purchased from Sigma Aldrich Chemical Co. (Milwaukee, WI).

Animals and Housing. All of the experimental protocols were in accordance with NIH guidelines and approved by the Institutional Animal Care and Use Committees of the Massachusetts Institute of Technology and Ohio State University. Male F344 rats, 4–5 weeks of age, were obtained from Harlan Sprague Dawley (Indianapolis, IN) and housed at Ohio State University. The animals were kept three per cage at 20 ± 2°C ambient temperature, 50 ± 10% relative humidity, and in a 12-h light/dark cycle. Twice weekly cage changes ensured maintenance of hygienic conditions. The animals were allowed to acclimate to the facility for 2 weeks before randomization into experimental treatment groups. The diet consisted of modified AIN-76A containing 20% casein, 0.3% D,L-methionine, 52% cornstarch, 13% dextrose, 5% cellulose, 5%

Received 11/25/02; accepted 4/28/03.

The costs of publication of this article were defrayed in part by the payment of page charges. This article must therefore be hereby marked *advertisement* in accordance with 18 U.S.C. Section 1734 solely to indicate this fact.

[1] Supported by grants from Hamamatsu Corp., the National Science Foundation (CHE-0111370), and the NIH through the National Center for Research Resources (P41-RR02594) and National Cancer Institute (CN15011-72). A. Wax was supported by a National Research Service Award fellowship grant from the NIH (F32 RR05075).

[2] To whom requests for reprints should be addressed, at Department of Biomedical Engineering, Box 90281, Duke University, Durham, NC 27708. Phone: (919) 660-5143; Fax: (919) 684-4488; E-mail: a.wax@duke.edu.

[3] The abbreviations used are: LSS, light-scattering spectroscopy; a/LCI, angle-resolved low-coherence interferometry; NMBA, *N*-nitrosomethylbenzylamine; FD, fractal dimension; AIN, American Institute of Nutrition; DFMO, difluoromethylornithine; POH, perillyl alcohol; LGD, low-grade dysplasia; HGD, high-grade dysplasia.

Table 1 *Protocol for administration of carcinogens and chemopreventives in the a/LCI study of rat esophagus epithelium*

Group	No.	Treatment	Amt. (ml)	Dose (mg/kg/b.w.)	Diet
1	4	DMSO + H_2O	0.2	0	Control AIN-76A
2	8	NMBA	0.2	0.25	Control AIN-76A
3	4	None	0	0	AIN-76A + DFMO (1000 ppm) Wk 6–25
4	8	NMBA	0.2	0.25	AIN-76A + DFMO (1000 ppm) Wk 6–25
5	4	None	0	0	AIN-76A + POH (1% w/w) Wk 6–25
6	8	NMBA	0.2	0.25	AIN-76A + POH (0.5% w/w) Wk 6–25
7	6	NMBA	0.2	0.25	AIN-76A + POH (1% w/w) Wk 6–25

corn oil, 3.5% AIN salt mixture, 1% AIN vitamin mixture, and 0.2% choline bitartrate (Dyets, Bethlehem, PA). Yellow lights were used in rooms where the animals were housed, because the chemopreventive agent, DFMO, is light sensitive. Food and water were available *ad libitum*.

Experimental Protocol. Carcinogen-treated animals (Table 1, *Groups 2*, *4*, *6*, and *7*) were given s.c. injections of NMBA (0.25 mg/kg body weight) in the intrascapular region three times a week for 5 weeks with concentrations adjusted weekly based on average body weight. The solvent for NMBA was 20% DMSO:H_2O, and the injection volume was 0.2 ml. A control group (Group 1) received a similar injection regimen of 20% DMSO:H_2O. At 25 weeks after the initial injection of NMBA, NMBA-treated and control rats were shipped to Massachusetts Institute of Technology to be harvested for optical spectroscopic analysis. The rats were euthanized by CO_2 asphyxiation and subjected to gross necropsy. The entire esophagus was excised and opened longitudinally for immediate optical spectroscopic analysis. After spectroscopic analysis, the esophagus was fixed in 10% neutral buffered formalin.

Chemopreventive Agents. Selected groups of rats were administered the chemopreventive agents DFMO (1000 parts/million) or POH (0.5 or 1%) in modified AIN-76A diet beginning 1 week after cessation of NMBA treatment until the end of the experiment (25 weeks). The diet containing DFMO was prepared weekly, and the diets with POH were prepared three times per week. Diets containing chemopreventive agents were stored at 4°C before administration to the animals.

a/LCI. Intact *ex vivo* tissue samples were scanned using the a/LCI technique (2, 5, 6). The measured a/LCI spectra consist of the angular distribution of scattered light, which contains information about the tissue structure, as a function of depth within the tissue. The light scattered from a particular depth is selectively detected using coherence gating. The effects of scattering by layers superficial to those of interest have been discussed previously (5) and are negligible for the selected depth of 50–80 μm in the present studies, corresponding to the basal cell layer of the esophageal epithelium. The basal layer is identified by the topmost sharp peak in the density profile of the tissue, obtained by angle integrating the a/LCI spectra. The diameter of the probe beam was 400 μm, which samples a few hundred cells at once, providing an average nuclear morphology in the probe volume. The use of an average minimizes the effect of variations in nuclear morphology from cell to cell, such as irregular nuclear shape and variations in density arising from differing phases of the reproductive cycle.

The a/LCI spectra from the basal cell layer of each sample was processed and analyzed to determine the average size, *i.e.*, diameter, of the cell nuclei, as described previously (2). In brief, a/LCI spectra consist of an oscillatory component superposed on a slowly varying background. The slowly varying feature of the a/LCI spectra was modeled using a low-order polynomial and removed. The resulting oscillatory component was then compared with a database of theoretical predictions obtained using Mie theory, from which the slowly varying features were similarly removed for analysis. The theoretical predictions were calculated for a Gaussian distribution of sizes characterized by a mean diameter (d) and SD (δD). In addition, the refractive index of the nuclei relative to the cytoplasm was varied from 1.015 to 1.072 in 36 discrete steps. The a/LCI technique was most sensitive to changes in mean nucleus size, and this parameter was the focus of the study; however, useful information was also obtained from the δD and refractive index measurements.

On obtaining the nuclear size distribution, the total Mie theory prediction for the determined size distribution was subtracted from the measured a/LCI spectrum. The resulting background component was then Fourier transformed

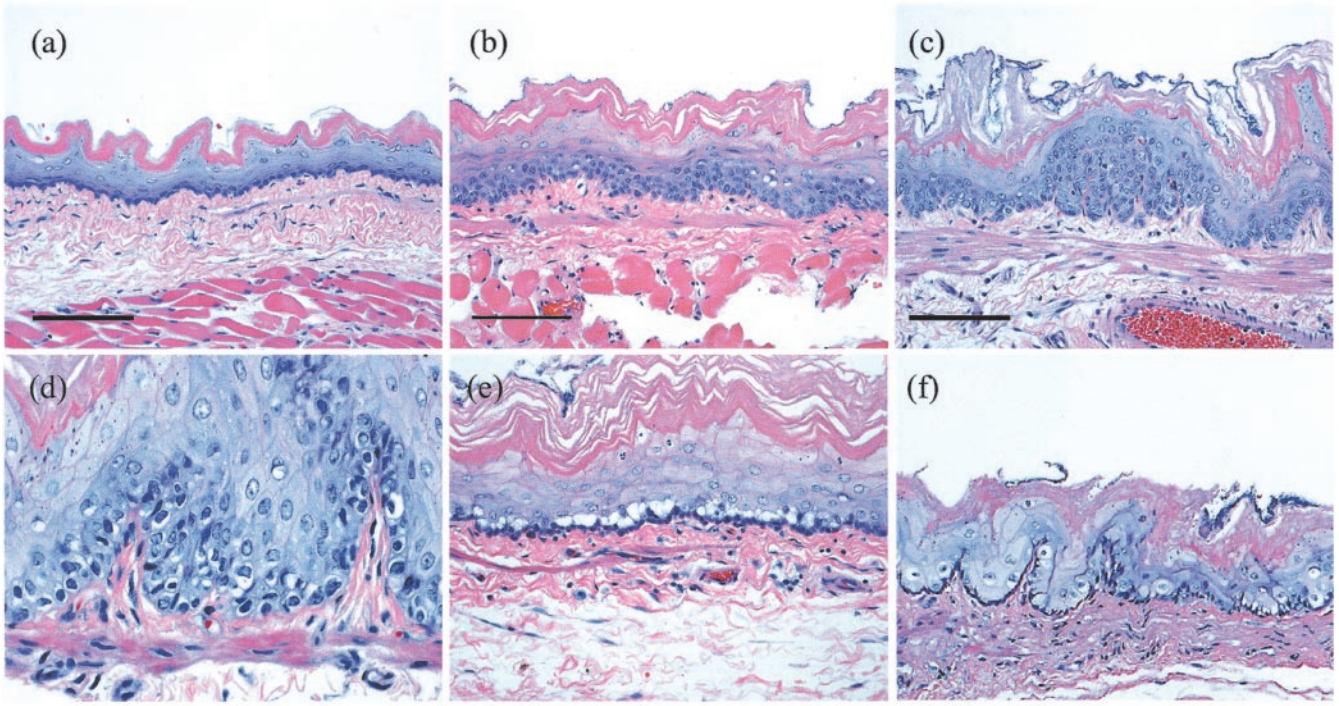

Fig. 1. Photomicrographs of fixed and stained esophagus sections illustrating the classification scheme (bar = 100 μm). Typical example of normal epithelium (*a*), LGD (*b*), HGD (*c*), epithelium with apoptotic bodies (*d*), and epithelium with vacuolated cells (*e*). The photomicrograph shown in *f* shows a case which was classified as containing apoptotic bodies but which also contained a significant number of normal epithelial cells.

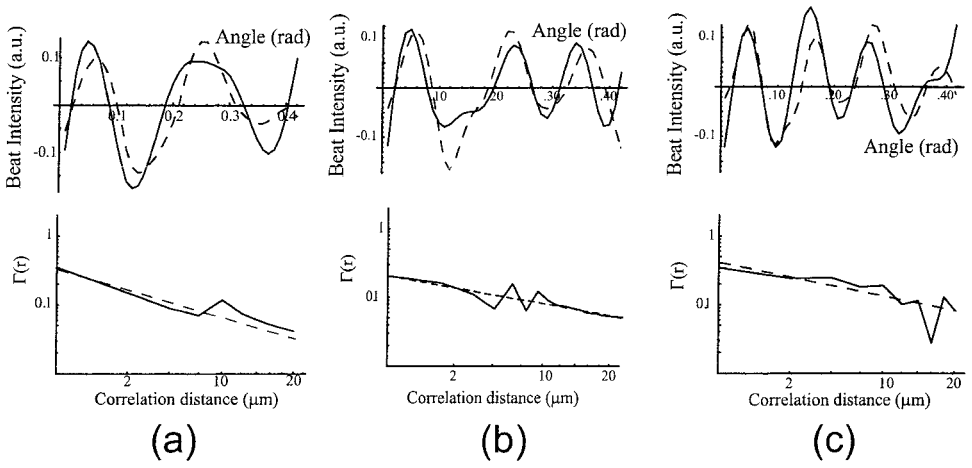

Fig. 2. Typical a/LCI spectra for several tissue types. In each case, the top graph shows the oscillatory component of the a/LCI spectrum (*solid line*) and fit to Mie theory (*dashed line*), and the bottom graph shows the correlation function (*solid line*) obtained from the background distribution and the power law fit (*dashed line*). *a*, normal epithelium: upper fit yields a mean size D = 9.8 μm, SD δD = 0.3 μm, and relative refractive index n = 1.43/1.37 = 1.044; lower fit yields FD = 2.06. *b*, LGD, upper fit yields a mean size D = 10.5 μm, SD δD = 0.26 μm, and relative refractive index n = 1.44/1.37 = 1.051; lower fit yields FD = 2.42. *c*, HGD, upper fit yields a mean size D = 14.4 μm, SD δD = 0.74 μm, and relative refractive index n = 1.44/1.37 = 1.051; lower fit yields D = 2.36.

to yield the two point correlation function, $\Gamma(r)$, with r the correlation distance. The general form of $\Gamma(r)$ for the tissue samples was a power law of the form $1/r^{\alpha}$, as indicated by its appearance as a straight line on a log-log plot. The parameter, α, was determined by a least squares fit to the data and related to the FD of these structures by $\alpha = 3 - \text{FD}$ (2). The use of the FD allows a physical interpretation of this measurement as the texture of the subcellular components (7). Larger FD corresponds to a denser, grainier distribution, whereas smaller FD indicates a smoother, finer distribution of structures. For each sample, both the size of the cell nuclei and their FD are reported.

Histological Grading of Neoplastic Tissues. Each esophagus was opened longitudinally, and the flat strip was cut into thirds and paraffin embedded with the epithelium uppermost. Longitudinal sections (4 μm) of each esophagus were cut, mounted on a microscope slide, and stained with H&E. The region corresponding to the area scanned using a/LCI was identified by measuring its location relative to the muscle gap at the tracheal junction of the esophagus. This region was then classified histologically as follows: (*a*) normal epithelium; (*b*) LGD; (*c*) HGD; (*d*) epithelium with vacuolated cells; or (*e*) epithelium with apoptotic cells (Fig. 1). This classification scheme was based on microscopic descriptions of dysplasia, vacuolated cells, and apoptosis given in Cotran *et al.* (8).

RESULTS

a/LCI Spectra. Typical measured a/LCI spectra for normal epithelium, LGD, and HGD are shown in Fig. 2. Each of the a/LCI spectra is shown as two parts: (*a*) the oscillatory component (upper) and (*b*) the correlation function obtained from the background distribution (lower). The oscillatory component is shown with the best fit from Mie theory, which determines the size of the cell nuclei. The correlation function is compared with the best fit power law as determined using a χ^2 fit. For each sample, two nuclear morphology parameters are reported: (*a*) the mean size of the cell nuclei and (*b*) the corresponding FD.

The a/LCI-measured morphological parameters, and the corresponding histological classifications, are presented graphically in Fig. 3. The data in Fig. 3*a* indicate an increase in mean nuclear size with neoplastic progression. The average nuclear size in normal tissues is 9.55 $\pm$ 0.23 μm. It increases to 10.5 $\pm$ 0.56 μm for LGD and 14.4 $\pm$ 0.21 μm for HGD. A statistically significant difference was found between the normal and LGD mean sizes ($P < 0.001$) and between normal and abnormal (LGD + HGD) mean sizes ($P < 0.005$). A decision threshold (dashed line), established using logistic regression, provides an 80% sensitivity and 100% specificity in distinguishing normal and dysplastic tissues, as indicated by the dashed line in Fig. 3*a*. The data in Fig. 3*b* show that there is also an increase of FD with neoplastic progression. The mean FD of the normal tissues was 2.05 $\pm$ 0.18 and increased to 2.28 $\pm$ 0.17 for abnormal tissues, a statistically significant difference ($P < 0.05$).

Samples showing cellular vacuolation associated with POH treatment also indicate an increase in mean nuclear size (13.2 $\pm$ 0.9 μm) but are indistinguishable from the dysplastic samples using this measurement. However, the FD in these samples decreased to 0.37 $\pm$ 0.2, in sharp contrast to the dysplastic tissues. For all samples with apoptotic cells, the data indicate a decrease in mean nuclear size (6.88 $\pm$ 0.9), but the FD remains comparable with that of normal tissues (2.03 $\pm$ 0.29). However, eliminating samples exhibiting both apoptotic cells and normal cells from this average calculation (as determined from histology), the mean nuclear size decreases to 6.52 $\pm$ 0.78, and the FD increases to 2.28 $\pm$ 0.17, a statistically significant ($P < 0.05$) difference from the average FD of normal samples.

Histological Grading. In total, 42 samples were examined. Each sample was classified in one of the five categories described above, and the results are summarized in Table 2. In the control group (Group 1), all tissue samples had a single layer of basal epithelial cells typical of normal rat esophagus. For samples treated with NMBA only (Group 2), tissues were classified as normal (25%), LGD (37.5%), and HGD (25%), with one sample classified as apoptotic. Group 3 served as the control group for the chemopreventive agent, DFMO, and all tissues appeared normal. Group 4 samples were treated with carcinogen (NMBA) and DFMO; the tissues were classified as normal (25%), LGD (50%), and apoptotic (25%). Group 5 was the control group for POH treatment, with tissues classified as normal (50%), apoptotic (25%), and vacuolated (25%). Group 6 samples were treated with NMBA and low-dose (0.5% w/w) POH, and tissues were classified as normal (25%), LGD (12.5%), apoptotic (37.5%), and vacuolated (25%). Group 7 samples received NMBA and high-dose (1%) POH, with tissues classified as normal (16.7%), apoptotic (66.7%), and vacuolated (16.7%). The average morphometric

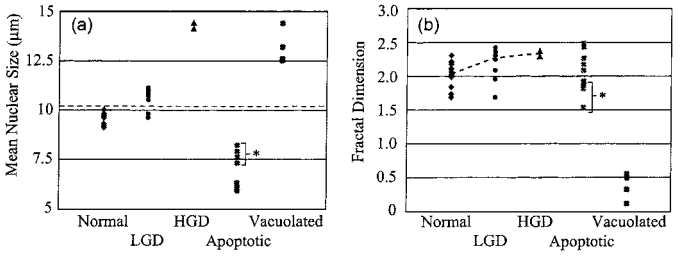

Fig. 3. *a*, average cell nuclei size determined with a/LCI. *Dashed line*, a decision line between normal and dysplastic cells. The points in the apoptotic classification marked with an *asterisk* indicate samples with normal cells also present, as shown in Fig. 1*f*. *b*, FDs of subcellular components measured using a/LCI. There is a significant difference ($P < 0.05$) between normal and dysplastic (*LGD + HGD*) populations. Trend line indicates changes in mean values of FD with neoplastic transformation. A significant difference is also seen between normal and apoptotic populations ($P < 0.05$) provided that the mixed classification samples (*asterisk*) are excluded.

Table 2 *Histological classification of rat esophagus samples, given as the number of samples exhibiting the classification per group as defined in Table 1*[a]

Group	Normal	LGD	HGD	LGD + HGD	Apoptotic	Vacuolated
1	4	0	0	0	0	0
2	2	3	2	5	1	0
3	4	0	0	0	0	0
4	2	4	0	4	2	0
5	2	0	0	0	1	1
6	2	1	0	1	3	2
7	1	0	0	0	4	1
Total	17	8	2	10	11	4
Mean size (μm)	9.55 ± 0.23	10.5 ± 0.56	14.3 ± 0.21	11.3 ± 1.6	6.88 ± 0.9	13.2 ± 0.9
Fractal dimension	2.05 ± 0.18	2.24 ± 0.16	2.32 ± 0.16	2.28 ± 0.17	2.03 ± 0.29	0.37 ± 0.2

[a] The summary shows the number of each classification and average nuclear morphology for that class.

parameters (mean nuclear size and FD) as measured by a/LCI are reported for each classification in Table 2.

DISCUSSION

The present study evaluated nuclear morphology in a rat model of esophageal carcinogenesis using a new optical tool, a/LCI. We measure the mean size of cell nuclei, as well as the average texture of the nuclei, parameterized by the FD, in the basal epithelial layer. These measurements were carried out in freshly excised, intact tissue samples without the need for staining agents or fixation.

Mean nuclear size is seen to be a powerful indicator of neoplastic progression, resulting in 80% sensitivity and 100% specificity in distinguishing normal from dysplastic tissues. Although including the FD measurements does not improve the diagnostic capability of the technique for classifying neoplasia, the measurements reveal important features of neoplastic progression and allow vacuolation to be distinguished from neoplasia.

The change in the background component of the a/LCI signals, which were interpreted as an increase in FD, arises from corresponding changes in the structural composition of the cells and tissues in the 2–10-μm size range as they undergo neoplastic transformation. The correlation function, $\Gamma(r)$, of the tissues reveals that this change corresponds to a decrease in smaller structures and an increase in larger structures. In the mass fractal model, an increase in FD is associated with a structure that visually appears thicker and clumped. Thus, the change in morphology for the dysplastic tissues revealed by the measured increase in FD agrees nicely with changes in the texture of cell nuclei seen in histological images, where clumped, grainy cell nuclei are characteristic of dysplasia. It is possible that the measured increase in FD results from changes in the organization of chromatin and proteins within the nucleus, as evidenced by the change in visual appearance of the cell nuclei in histological images.

This study also examined the effects of chemopreventive agents by measuring changes in cellular morphometry. Both DFMO and POH were seen to induce apoptosis in the samples. The a/LCI measurements showed a decrease in mean nuclear size and an increase in FD, both features agreeing with the contracted nucleus seen in apoptosis. This is good evidence of the chemopreventive action occurring by inducing apoptosis to alter the proliferative status of the epithelial cells. Indeed, the average size of esophageal tumors (papillomas) in rats treated with NMBA + DFMO and in those treated with POH + DFMO was found to be significantly smaller than that in rats treated with NMBA only; an observation consistent with an increased rate of apoptosis in DFMO- and POH-treated animals (9).

In several of the esophageal samples from animals treated with POH, the basal epithelial cells were found to be vacuolated. POH has been shown to elicit toxicity in animals (10) and humans (11), and animals treated with POH in our study had >10% weight loss indicative of toxicity (9). In many cases, the vacuolated cells appeared to be devoid of nuclei. Thus, the a/LCI measurement yields the average size of the vacuoles, which was measured to be larger than the size of the cell nuclei in normal tissues. Although these measurements alone are insufficient to distinguish vacuoles from dysplastic cells, which also exhibit increased nuclear size, the FD measurements are markedly different. For the vacuolated cells, the FD drops significantly, agreeing well with the voided appearance of the vacuoles. The presence of the vacuoles indicates a toxicity effect of POH on the esophagus, which may limit its efficacy as a chemopreventive agent (9).

The ability of a/LCI to measure nuclear morphometry *in situ* makes it a powerful tool for assessing neoplastic transformation. The a/LCI technique can also distinguish unusual tissue states, such as apoptosis and vacuolation, permitting investigations of the efficacy of chemopreventive agents or the toxic effects of chemicals. Further refinement of the technique is expected to permit rapid scanning of multiple fields in a tissue sample, greatly increasing its applicability. The measurement of nuclear texture via the FD provides a unique probe of cellular characteristics. It will be interesting to see how FD impacts the understanding of cancer biology.

ACKNOWLEDGMENTS

We thank Vadim Backman for interpreting FDs and Irene Georgakoudi for statistical analysis.

REFERENCES

1. Backman, V., Wallace, M. B., Perelman, L. T., Arendt, J. T., Gurjar, R., Muller, M. G., Zhang, Q., Zonios, G., Kline, E., McGillican, T., Shapshay, S., Valdez, T., Badizadegan, K., Crawford, J. M., Fitzmaurice, M., Kabani, S., Levin, H. S., Seiler, M., Dasari, R. R., Itzkan, I., Van Dam, J., and Feld, M. S. Detection of preinvasive cancer cells. Nature, *406:* 35–36, 2000.
2. Wax, A., Yang, C., Backman, V., Badizadegan, K., Boone, C. W., Dasari, R. R., and Feld, M. S. Cell organization and sub-structure measured using angle-resolved low coherence interferometry. Biophys. J., *82:* 2256–2264, 2002.
3. Izatt, J. A., Kulkarni, M. D., Wang, H. W., Kobayashi, K., and Sivak, M. V. Optical coherence tomography and microscopy in gastrointestinal tissues. IEEE Journal of Selected Topics in Quantum Electronics, *2:* 1017–1028, 1996.
4. Huang, D., Swanson, E. A., Lin, C. P., Schuman, J. S., Stinson, W. G., Chang, W., Hee, M. R., Flotte, T., Gregory, K., Puliafito, C. A., and Fujimoto, J. G. Optical coherence tomography. Science, *254:* 1178–1181, 1991.
5. Wax, A., Yang, C., Backman, V., Kalashnikov, M., Dasari, R. R., and Feld, M. S. Determination of particle size using the angular distribution of backscattered light as measured with low-coherence interferometry. J. Opt. Soc. Am. A, *19:* 737–744, 2002.
6. Wax, A., Yang, C. H., Dasari, R. R., and Feld, M. S. Measurement of angular distributions by use of low-coherence interferometry for light-scattering spectroscopy. Optics Letters, *26:* 322–324, 2001.
7. Einstein, A. J., Wu, H. S., and Gil, J. Self-affinity and lacunarity of chromatin texture in benign and malignant breast epithelial cell nuclei. Phys. Rev. Lett., *80:* 397–400, 1998.
8. Cotran, R. S., Robbins, S. L., and Kumar, V. (eds.). Robbins Pathological Basis of Disease. Philadelphia: Saunders, 1994.
9. Liston, B. W., Nines, R., Carlton, P. S., Gupta, A., Aziz, R., Frankel, W., and Stoner, G. D. Evaluation of perillyl alcohol as a chemopreventive agent in *N*-nitrosomethylbenzylamine (NMBA)-induced rat esophageal tumorigenesis. Cancer Res., *10:* 2399–2403, 2003.
10. Evans, E., Arneson, D., Kovatch, R., Supko, J., Morton, T., Siemann, L., Cannon, J., Tomaszewski, J., and Smith, A. Toxicology and pharmacology of perillyl alcohol (NSC-641066) in rats and dogs. Proc. Am. Assoc. Cancer Res., *36:* 366, 1995.
11. Ripple, G. H., Gould, M. N., Stewart, J. A., Tutsch, K. D., Arzoomanian, R. Z., Alberti, D., Feierabend, C., Pomplun, M., Wilding, G., and Bailey, H. H. Phase I clinical trial of perillyl alcohol administered daily. Clin. Cancer Res., *4:* 1159–1164, 1998.